

Citation for published version:

Hussain, A, Calabria-Holley, J, Lawrence, M, Ansell, MP, Jiang, Y, Schorr, D & Blanchet, P 2019, 'Development of novel building composites based on hemp and multi-functional silica matrix', *Composites Part B: Engineering*, vol. 156, pp. 266-273. <https://doi.org/10.1016/j.compositesb.2018.08.093>

DOI:

[10.1016/j.compositesb.2018.08.093](https://doi.org/10.1016/j.compositesb.2018.08.093)

Publication date:

2019

Document Version

Peer reviewed version

[Link to publication](#)

Publisher Rights

CC BY-NC-ND

University of Bath

Alternative formats

If you require this document in an alternative format, please contact:
openaccess@bath.ac.uk

General rights

Copyright and moral rights for the publications made accessible in the public portal are retained by the authors and/or other copyright owners and it is a condition of accessing publications that users recognise and abide by the legal requirements associated with these rights.

Take down policy

If you believe that this document breaches copyright please contact us providing details, and we will remove access to the work immediately and investigate your claim.

Development of novel building composites based on hemp and multi-functional silica matrix

Atif Hussain^{a, b,*}, Juliana Calabria-Holley^a, Mike Lawrence^a, Martin P. Ansell^a, Yunhong Jiang^a, Diane Schorr^b, Pierre Blanchet^b

^aBRE Centre for Innovative Construction Materials, Department of Architecture and Civil Engineering, University of Bath, Bath BA2 7AY, UK

^bDepartment of Wood and Forest Sciences, Université Laval, Quebec, QC, G1V 0A6, Canada

*Corresponding Author: Atif Hussain (A.Hussain@bath.ac.uk)

Abstract

This study focuses on the development of novel bio-composites using a silica matrix that provides dual functionality: as a hydrophobic surface treatment and as a binder for hemp-shiv. The hydrophilic nature of hemp shiv, a plant based aggregate, results in composites having poor interfacial adhesion, weak mechanical properties and long drying times. In this work, sol-gel process has been utilised to manufacture durable low density hemp based composites. Morphological characterisation by scanning electron microscopy (SEM) showed that hemp shiv was embedded well in the matrix. Detailed chemical analysis using x-ray photoelectron spectroscopy (XPS) and gas chromatography-mass spectrometry (GC-MS) indicate the presence of water soluble and ethanol soluble extractives leached from the hemp shiv which are incorporated into the silica matrix inducing the binding effect. The composites were water resistant and showed good mechanical performance having the potential to develop novel thermal insulation building materials.

Keywords

Hemp; B. Adhesion; D. Chemical analysis; Mechanical testing

1. Introduction

Bio-based materials have become increasingly popular for producing economical engineering materials in the building and construction industry. Composites manufactured using the woody core of the hemp plant (*Cannabis Sativa* L.) known as shiv have been adopted by the building industry. Lightweight composites from hemp shiv possess excellent hygroscopic [1,2], thermal [3,4] and biodegradable [5] properties.

Hemp shiv has low density due to its high porosity and it tends to absorb large amounts of water [6]. The hydrophilic nature of bio-based materials makes them incompatible with hydrophobic thermoset/thermoplastic polymers [7]. On the other hand, since the shiv competes with the binder for the available water, purely hydraulic binders like lime or cement cannot hydrate completely, leading to a powdery inner core in the hemp-lime walls which is poorly bound [8]. The issue of adhesion with hemp-lime has stimulated considerable investment in hemp-specific lime based binders. The most recent generation of binders utilises high specific surface area lime in order to obtain a more reactive binder, however, they are still susceptible to adhesion issues. Pre-fabrication of panels or blocks ensures factory controlled conditions which reduce the extremes of adhesion issues (e.g. extensive flouring), but there still remains the inherent issue that the soluble sugars on the surface of the shiv interfere with the hydration of the binders, resulting in lower strength composites [9]. The durability of the material is compromised due to high moisture uptake as colonial fungal growth is encouraged resulting in cell wall degradation [10].

The major constituents of industrial hemp shiv are: cellulose (44%), hemicellulose (18-27%), lignin (22-28%) and other components such as extractives (1-6%) and ash (1-2%) [11,12]. Extractives include numerous low molecular mass compounds such as fatty acids, waxes, sterols, triglycerides, steryl esters, glycosides, fatty alcohols, terpenes, phenolics, simple sugars, alkaloids, pectins, gums and essential oils. It is well known that extractives can be isolated using polar and non-polar solvents. Volatile extractives are represented by highly volatile compounds which can be separated by water distillation. They are mainly composed of monoterpenes and other volatile terpenes including terpenoids as well as many different low

molecular weight compounds. Water-soluble compounds consist of various phenol compounds, carbohydrates, glycosides and soluble salts, which can be extracted by cold or hot water [13–15]. Lipophilic extractives are insoluble in water but soluble in organic solvents such as hexane, dichloromethane, diethyl ether, acetone or ethanol [16]. Lipophilic extractives also known as plant-resins are divided into free acids, e.g. resin acid and fatty acid, and neutral compounds, e.g. fats and waxes. Extractives from bio-based materials can have a tacky nature forming pitch deposits which is considered to be a major problem in the paper and pulp industry [17].

Natural fibre composites have low durability and tend to absorb large amounts of moisture weakening interfacial adhesion and degradation, although this property can be improved by treatment of the fibres [18–20]. Physical approaches such as plasma, ultraviolet or corona treatment modify the fibre surface for enhancing roughness and interfacial adhesion. Chemical treatments such as alkaline, silane and acetylation offer better improvements than physical methods enhancing hydrophobicity and roughness of the fibres resulting in better interfacial bonding [20–24]. Addition of silica particles into polymeric matrix has also been used to enhance the mechanical properties of natural fibre reinforced composites [25]. Hydrolysed silanes can chemically attach to the hydroxyl group of fibres, but they are known to provide only a limited improvement in the mechanical properties of the resulting fibre composite due to their physical compatibility with the matrix. The strength of natural fibre composites can be increased if covalent bonds are present between the silane treated fibre and matrix [19,20]. Therefore there is a need to develop novel composites that possess good interfacial bonding and at the same time utilise the benefits of chemically treated bio-based aggregates being resistant to water and degradation.

The work reported in this paper is carried out under the ISOBIO project which aims to develop hygrothermally efficient bio-based building insulation panels with low embodied energy and low embodied carbon. We have previously reported that the silica based treatment can provide hydrophobicity to hemp shiv [26] without compromising its moisture buffering capacity as the pores are not totally blocked by the coating [27]. The aim of this paper is to demonstrate the use

of a hydrophobic silica treatment as a binder for hemp shiv to produce novel robust light weight composites with enhanced water resistance.

2. Materials

Hemp shiv used in this study was received from CAVAC, an agricultural cooperative based in north-west France. Tetraethyl orthosilicate (TEOS, 98%), hexadecyltrimethoxysilane (HDTMS, 85%), nitric acid (70%) and absolute ethanol were obtained from Sigma-Aldrich.

2.1 Silica formulation and preparation

The silica based binder was synthesised by hydrolysis and condensation of TEOS in ethanol and water. The reaction was catalysed by nitric acid. For the preparation of the silica, 1M of TEOS was added to a mixture of 4M distilled water, 4M of absolute ethanol and 0.005M of nitric acid. 0.015M of HDTMS was added to the above mixture as the hydrophobic agent. The sol was vigorously stirred at 40 °C and atmospheric pressure for nearly 2 hours. The sols were allowed to age for 96 hours in closed container at room temperature.

For the preparation of the silica glass, the sol was aged in a container at room temperature until the gel point was reached. The gel-point was taken as the time when the sol did not show any movement on turning the container upside down. For analysis of the binder, the left-over sol contaminated with leached out hemp shiv extractives was aged in a container until the gel point was reached and the specimen was termed the “binding matrix”. A schematic illustration of silica glass has been presented in Figure 1.

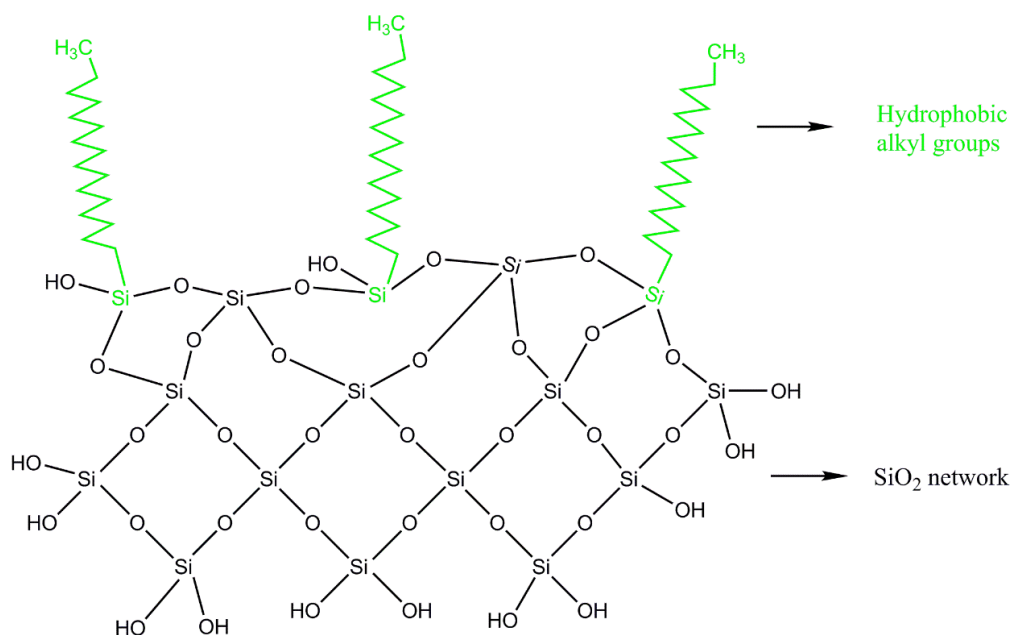


Figure 1. Schematic illustration of the silica glass.

2.2 Binder characterisation

The surface morphology of the specimens was characterised using a scanning electron microscope (SEM), JEOL Corporation Model SEM-6480LV (Tokyo, Japan) operating at an accelerating voltage of 10 kV. The specimens were coated with gold using an HHV500 sputter coater (Crawley, UK) to prevent charging and to achieve high quality images of morphological characteristics. Energy dispersive X-ray spectroscopy (Oxford INCA) was used to characterise the elemental composition of the specimens.

The surface elemental and chemical composition of the specimens were analysed using X-ray photoelectron spectroscopy (XPS). Prior to XPS analysis, samples were oven-dried at 80 °C for 96 hours. XPS spectra of the samples were recorded with an X-ray photoelectron spectrometer (Kratos Axis Ultra, UK). All spectra were collected using a monochromatic Al $\text{K}\alpha$ X-ray source operated at 300 watts. The lateral dimensions of the samples were 800 microns \times 400 microns, corresponding to spot size of the Al $\text{K}\alpha$ X-ray used, and probing depth was approximately 5 nanometres. For each sample, two spectra were recorded: (i) survey spectra (0–1150 eV, pass energy 160 eV, and step size 1 eV) recorded for apparent composition calculation; and (ii) high-resolution C1s, O1s and Si 2p spectra (within 20 eV, pass energy 20 eV and step size within

0.05eV) recorded to obtain information on chemical bonds. Calculation of the apparent relative atomic concentrations was performed with the CasaXPS software. Peak fitting was performed with CasaXPS, which automatically and iteratively minimizes the difference between the experimental spectrum and the calculated envelope by varying the parameters supplied in a first guess.

Thermal analysis of the samples was carried out by simultaneous thermogravimetric analysis (TGA) and differential scanning calorimetry (DSC) using the STA 449 F1 Jupiter thermal analyser (Netzsch, Germany). The specimens were heated at a rate of 10 °C/min from 25 to 950 °C under nitrogen atmosphere purged at 30 ml/min using an alumina crucible.

2.3 Extractive Analysis

For isolation of the extractives, oven dried hemp shiv pieces were immersed in a solution containing a mixture of ethanol and water in the molar ratio 1:1 to represent the solvent ratio used in the sol formulation. Extraction of the hemp shiv samples was done using Soxhlet apparatus for 2 h at 80 °C. The extract was evaporated to dryness using a rotary evaporator and placed overnight in a vacuum oven. The dried extract was re-suspended in hexane and methylene chloride for chromatographic analysis of the lipophilic fraction. Gas chromatography–mass spectrometry (GC-MS) analysis was performed on a Varian CP 3800 gas chromatograph coupled to a mass spectrometer detector (Varian Saturn 2000 MS/MS, 40-650 a.m.u.). The GC oven was kept at 50 °C for 5 min and then heated to 250 °C at 5 °C/min. The final temperature was held for 2 min. The injector temperature was set at 250 °C. Helium was used as the carrier gas at a flow rate 1.0 ml/min. 1 µl of oil (solvent extractive) was injected using a rear injector type 1177 with a split ratio 1:10. The spectrometer was operated in the electron impact mode using 30 µA emission current and mass range m/z 40-600. Peaks were quantified by area and the compounds were identified by comparing the mass spectra with those from Wiley and NIST computer libraries.

2.4 Preparation of composite samples

Mixing of the constituent materials, hemp shiv (75 vol%) and sol (25 vol%), were carried out manually to achieve a uniform mixture. The mass of the materials was pre-calculated to target a final density of 175 kg/m³ for the composites. Aggregates of hemp shiv were mixed with the sol and then placed into a phenolic ply mould, tamped down and left overnight in the oven at 80 °C. The specimens were removed from the moulds and transferred to a conditioning room at 19 °C and 50% relative humidity. Another set of samples were prepared by mixing hemp shiv (75 vol%) and ethanol-water solution (25 vol%) and rest of the conditions were kept constant as described above.

2.5 Composite characterisation

Compressive tests were conducted on 100mm cube samples using an Instron 50 KN testing rig at a controlled displacement rate of 3 mm/min; the inbuilt instrumentation was used to both record load and platen displacement at a resolution of one data point per 0.1 s. A durability test was performed to determine the robustness of the binder. Composite samples were fully immersed in water for 24 hours at 20 °C. The samples were removed from water and placed in an oven at 80 ° for complete drying until no further mass change was observed. Compression tests were performed on these samples and the results were compared with control samples. Prior to compression testing, the samples were placed in a conditioning room at 19 °C and 50% relative humidity for at least 24 hours. The tests were performed in triplicate and the average reading was reported.

3. Results

3.1 Morphology characterisation

The morphology of the silica glass, hemp shiv composite and the binding matrix is presented in Figure 2. The silica glass (figure 2A) has a smooth texture and is classically brittle when compared to the binding matrix (Figure 2B) which exhibits some spallation. In general, the hemp shiv particles are well embedded in the matrix due good interaction between the hemp shiv and binding matrix. However, some minor cracks appear in the matrix (Figure 2C) which could be a result of shrinkage during drying of the gel.

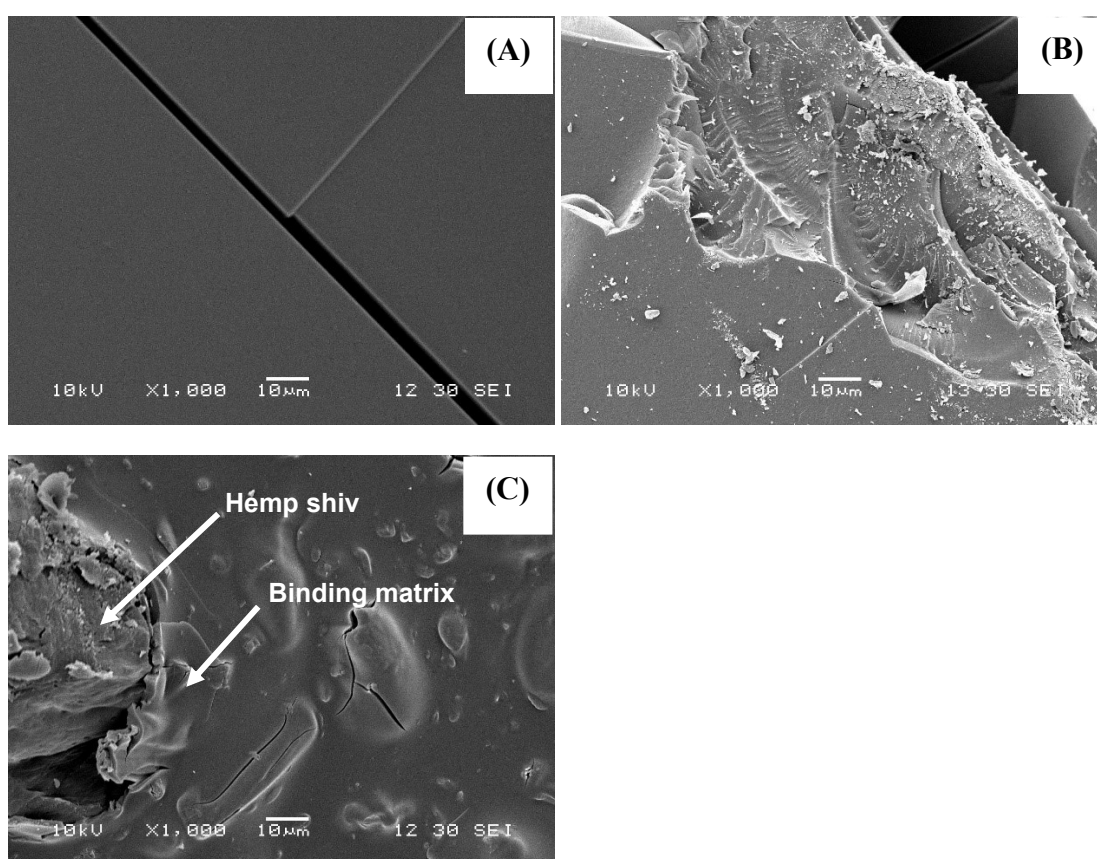


Figure 2. SEM micrographs of (A) silica glass, (B) binding matrix and (C) hemp shiv composite.

3.2 Chemical characterisation

The EDX analysis (Table 1) shows the surface composition of the silica specimens. The percentage of carbon is significantly higher in the binding matrix than the silica glass. The presence of carbon in the silica glass is due to the alkyl groups providing functionalisation.

Table 1. EDX analysis of silica glass and binding matrix.

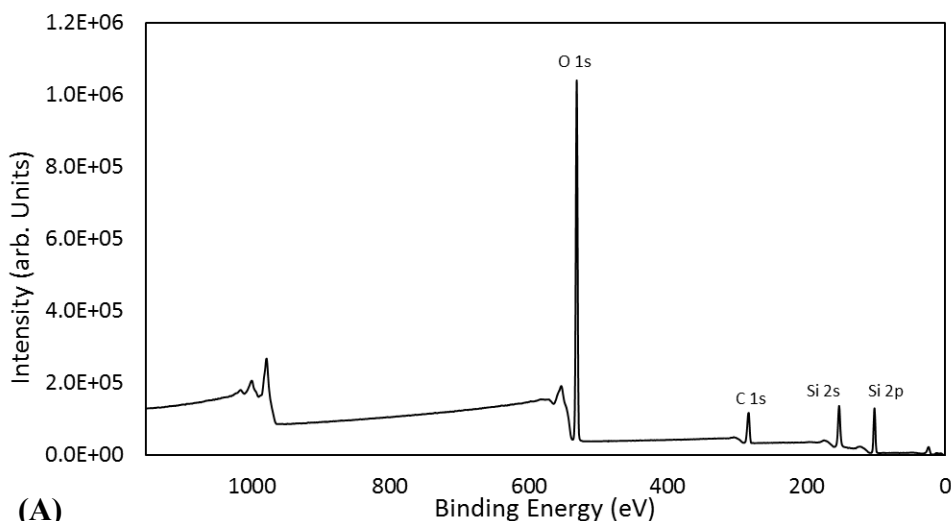
Element	Silica glass		Binding matrix	
	Weight %	Atomic %	Weight %	Atomic %
C K	19.41 ± 3.8	28.69 ± 4.5	51.45 ± 5.3	61.94 ± 4.9
O K	43.21 ± 3.3	51.07 ± 7.1	34.86 ± 3.2	31.65 ± 3.7
Si K	43.33 ± 7.6	29.48 ± 7.3	7.15 ± 1.8	3.71 ± 1.1
Other	0.35 ± 0.1	0.26 ± 0.1	6.54 ± 0.2	2.69 ± 0.2

The chemical composition of the silica glass and the binding matrix was determined by X-ray photoelectron spectroscopy. The atomic percentage of various elements present at the sample surface was determined by a low-resolution survey scan. The relative elemental composition for the specimens is listed in Table 2.

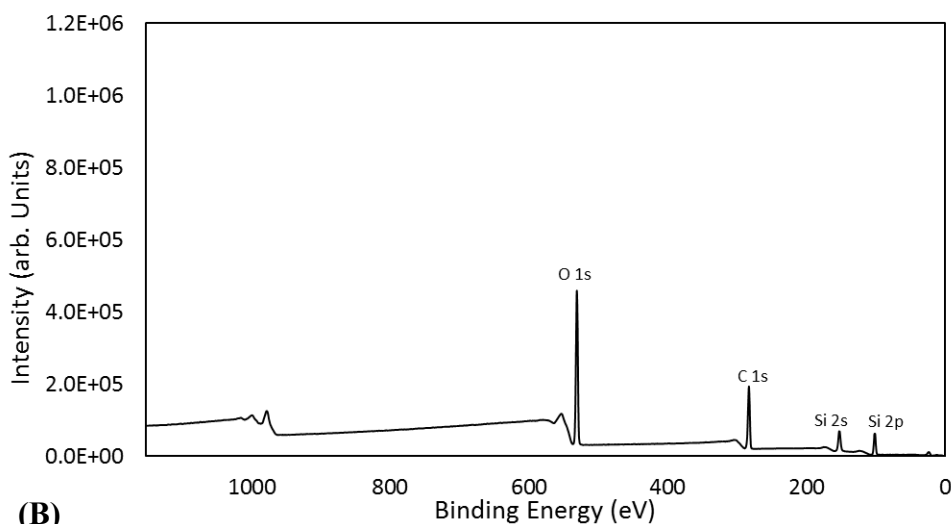
Table 2. Relative amount of atoms in the sample determined by low-resolution XPS scan.

Element	Relative Concentration (Atomic %)	
	Silica Glass	Binding matrix
C	19.86	46.09
O	61.50	40.34
Si	18.64	13.58

The main elements detected for both the silica specimens were carbon, oxygen and silicon. The binding matrix showed higher content of carbon as seen in Figure 3.



(A)



(B)

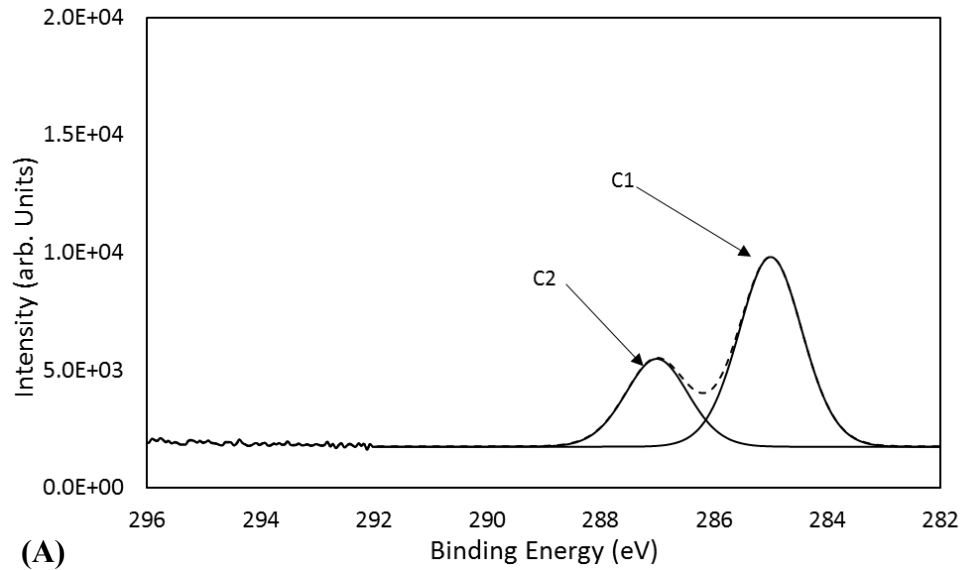
Figure 3. XPS survey scan for (A) silica glass, (B) binding matrix.

A high-resolution scan was performed on the C1s region for the silica glass and the binding matrix (Figure 4) to determine the type of oxygen-carbon bonds present. The chemical bond analysis of carbon was performed by curve-fitting the C1s peak and deconvoluting it into four sub peaks corresponding to unoxidized carbon C1, and various oxidized carbons C2, C3 and C4. The binding energy, corresponding bond type and their relative percentage are listed in Table 3. The silica based binder shows additional oxidised carbon sub peaks, C3 and C4.

Table 1. Deconvoluted peak parameters and relative amount of different carbon-to-oxygen bonds at sample surface determined by high-resolution XPS.

Carbon Group	Peak parameters		Relative amount (% area)	
	Binding Energy (eV)	Bond	Silica Glass	Binding matrix
C1	285.0	C-C or C-H	68.65	84.30
C2	286.6/286.8	C-OH	31.35	10.40
C3	288.0	O-C-O or C=O	0.00	4.50
C4	289.2	O-C=O	0.00	0.81

The C1s high resolution spectra with the deconvoluted peaks for silica glass and binding matrix are represented in Figure 4. The C1 peak is related carbon-carbon or carbon-hydrogen bonds whereas C2, C3, and C4 peaks are associated with carbon-oxygen bonds.



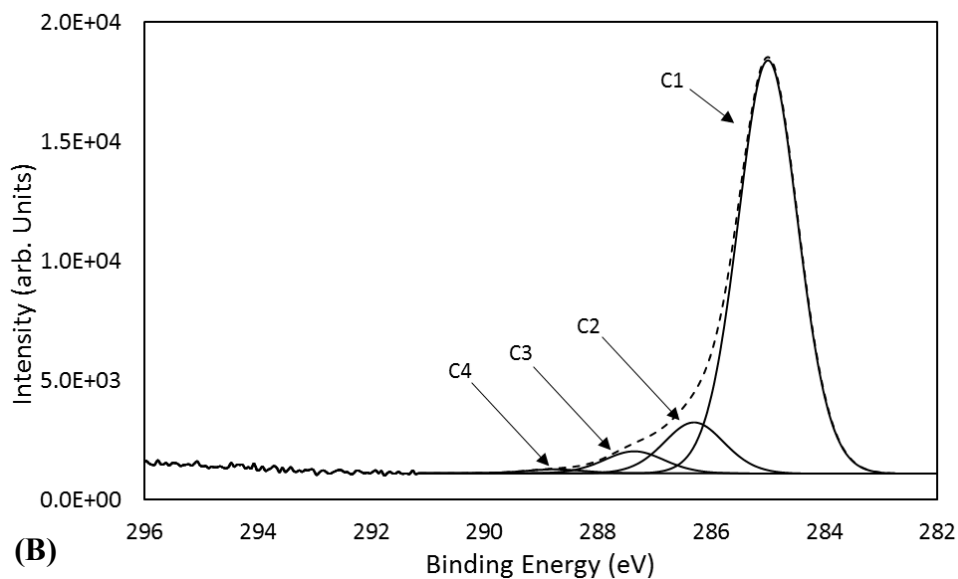
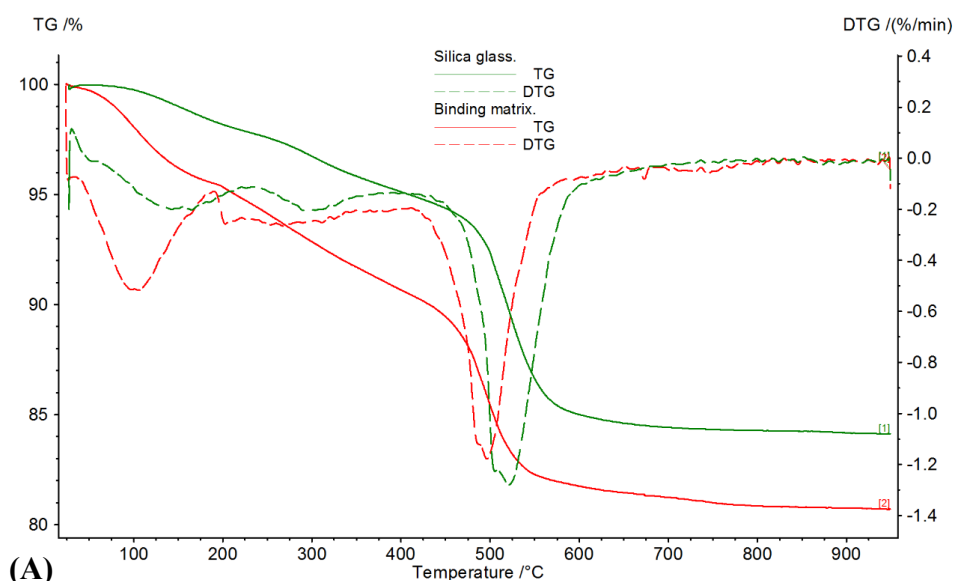
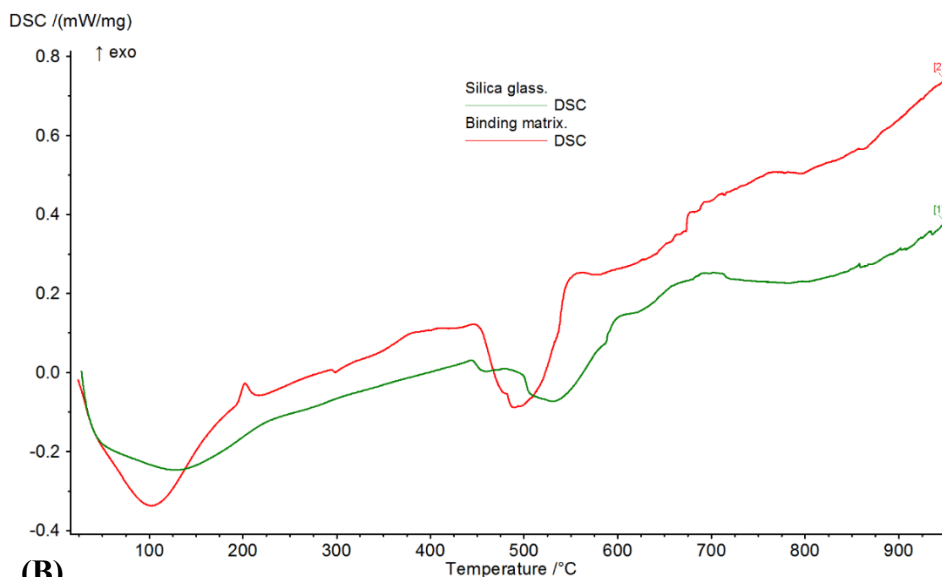


Figure 4. XPS scan of C1s region for (A) silica glass, (B) binding matrix.

3.3 Physical characterisation

The thermal analysis of the silica glass and the binding matrix is reported in Figure 5. From the TGA weight loss curves, it is seen that silica glass has a residual mass of 84.1% whereas the binding matrix has a residual mass of 80.7% at 950 °C. The maximum decomposition peak determined from the first derivative of the weight loss thermogram (DTG) curve is at 525 °C for silica glass and 495 °C for the binding matrix.





(B) Figure 5. Thermal analysis of silica glass and binding matrix; (A) TGA and DTG curves, (B) DSC curves.

The DSC graph of the binding matrix shows a stronger endothermic peak at 102 °C when compared to the endothermic peak at 128 °C for silica glass. The endothermic peaks corresponding to the maximum decomposition rate are at 489 °C and 530 °C for the binding matrix and silica glass respectively.

3.4 Identification of Extractives

The identification of the extracted compounds was performed using GCMS. The polar components of the extractives were analysed for identification of the lipophilic extractives which are responsible for their tacky nature [28] and would contribute to the adhesive properties of the binding matrix. The yield of total extractives (polar and non-polar) in hemp shiv was 6.23% (dry weight %). The hexane yield and methylene chloride yield in the total extract was 9.05% and 5.00% respectively.

The chromatographs for hexane extract and methylene chloride extract are presented in Figures 6 and 7 respectively. All the compounds identified by GCMS are listed in Tables 4 and 5. The individual compounds were identified based on a comparison with GC retention times and mass spectra from the NIST library. Over twenty compounds were identified in the hexane

extract and twelve compounds were identified in the methylene chloride extract. For the analysis of the GCMS data, peaks lower than 30000 counts were rejected. From the chromatograms, it was determined that fatty acids esters, mainly lauric acid and phthalic acid, gave the highest peaks.

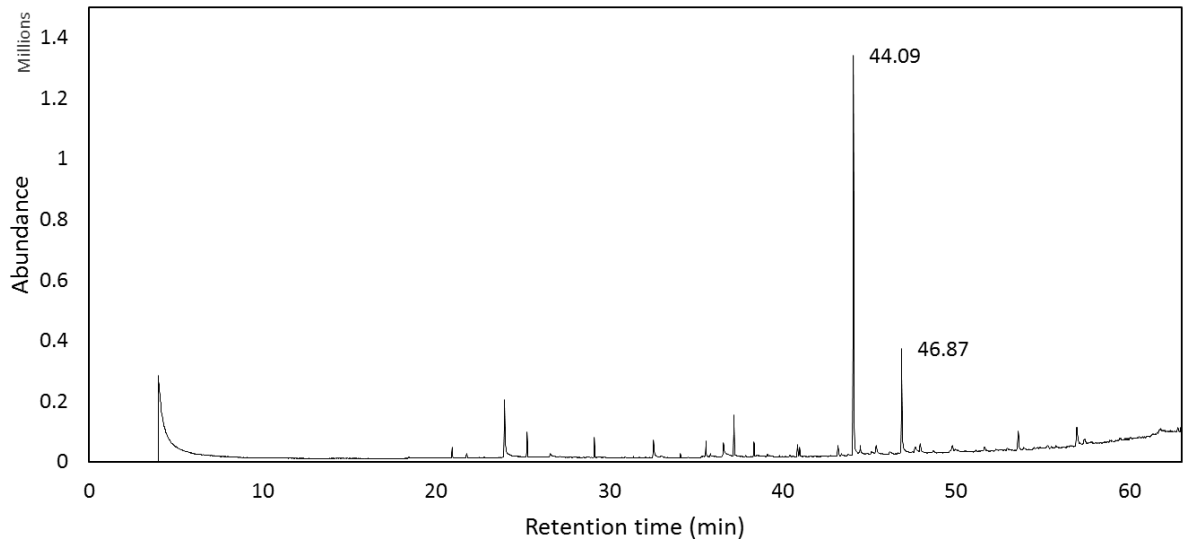


Figure 6. The chromatogram of hexane extractives from hemp shiv.

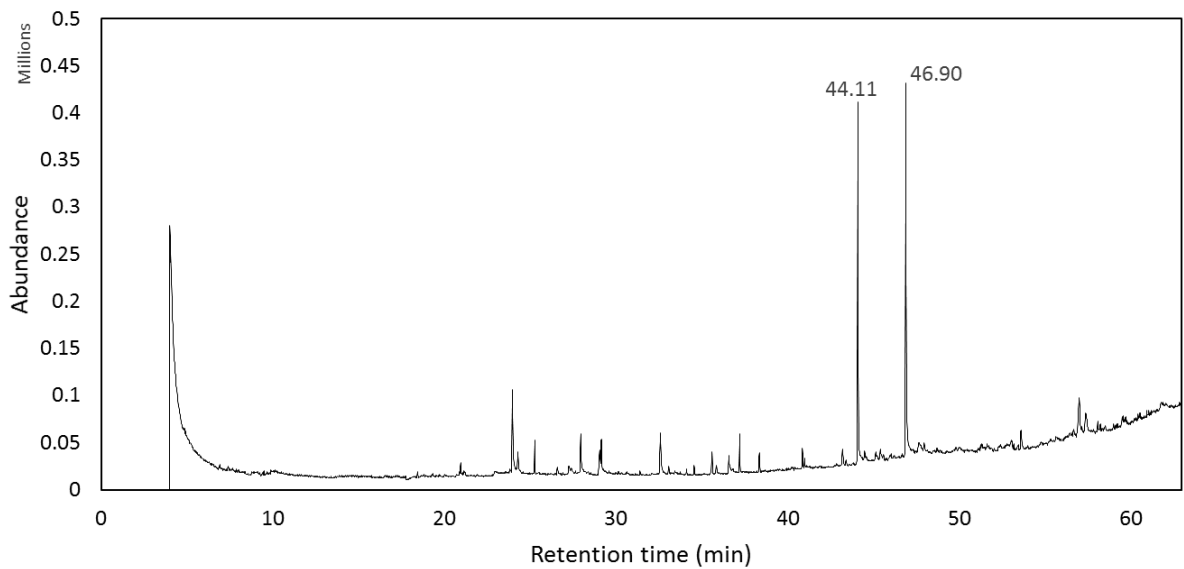


Figure 7. The chromatogram of methylene chloride extractives from hemp shiv.

276 Table 4. GCMS peak area and retention time of lipophilic extractives identified in hemp shiv
277 hexane extract.

Compound (Hexane Extract)	Retention time (min)	Peak Area
4-Hydroxy-3-nitrobenzaldehyde	23.961	732645
14-Methyl-8-hexadecen-1-ol	34.108	42090
Pentadecanoic acid	36.601	235957
Hexadecanoic acid, ethyl ester	37.202	346033
Heptadecanoic acid, 15-methyl-, ethyl ester	40.988	79364
Tetradecanal (Myristaldehyde)	43.402	32795
Dodecanoic acid (lauric acid), tetradecyl ester	44.086	4120000
Heptadecanoic acid, ethyl ester	44.484	94511
Oleyl alcohol	45.124	37702
1,2-Benzenedicarboxylic acid (phthalic acid), isodecyl octyl ester	46.872	1124000
Tricosanoic acid, methyl ester	47.939	159469
13-Heptadecyn-1-ol	48.691	31836
Tetracosanoic acid, methyl ester	49.676	33092
Eicosanoic acid	49.815	181870
Hexadecanoic acid, octadecyl ester	51.163	31625
Pentacosanoic acid, methyl ester	51.658	113374
Ergost-5-en-3-ol	52.97	48769
Tricosane	53.592	327306
9,19-Cyclocholestene-3,7-diol,4,14-dimethyl-,3-acetate	53.91	38821
Cholestra-4,6 dien-3-ol	55.287	88534
Stigmasterol	55.784	34398
7-Dehydrodiosgenin	56.974	371899
Stigmastan-3-ol, 5-chloro-, acetate, (3.beta.,5.alpha.)	57.416	91981
Stigmastan-3-ol, 5-chloro-, acetate, (3.beta.,5.alpha.)	57.447	81052

278

279

Table 5. GCMS peak area and retention time of lipophilic extractives identified in methylene chloride extract of hemp shiv.

Compound (Methylene Chloride Extract)	Retention time (min)	Peak Area
4-Hydroxy-3-nitrobenzaldehyde	23.97	450485
2,6-Dimethoxybenzoquinone	27.945	287931
4-Hydroxy-3-nitrobenzoic acid	29.049	93543
Phenol,2,4-dinitro-6-methoxy	32.602	216393
Pentadecanoic acid	36.589	65679
Hexadecanoic acid, ethyl ester	37.221	111908
Octadecanoic acid, ethyl ester	41.011	28187
Dodecanoic acid (lauric acid), tetradecyl ester	44.108	1.70E+06
1,2-Benzenedicarboxylic acid (phthalic acid), mono(2-ethylhexyl) ester	46.899	2.75E+06
Octadecane, 3-ethyl-5-(2-ethylbutyl)-	53.625	106470
Stigmasta-5, 22-dien-3-ol, acetate, (3.beta.)-	57.009	348774
Cholest-1-eno[2,1-a]naphthalene,3',4'-dihydro-	57.396	263327

3.5 Composite characterisation

The compression testing of the composite samples prepared with hemp shiv and binding matrix is imaged in Figure 8 and stress versus strain curves for the before and after immersion samples are presented in Figure 9. The moisture sensitivity of the composite was determined by comparing the mechanical properties of the hemp shiv composite before and after immersion in water for 24 hours. Preparation of composite samples using hemp shiv and ethanol-water solution (see section 2.4) was unsuccessful as the hemp shiv particles were not able to bind.

From Figure 9, the results from three test samples before immersion reveal that the composite reaches an average compressive stress of 0.48 ± 0.02 MPa at 30% strain. After the immersion test, a slight reduction in compressive stress by 15% was observed for the three samples and the average reading was 0.41 ± 0.01 MPa at 30% strain. It was noted that further compression led to densification of the sample. After compression, the sample showed some elastic behaviour as seen in Figure 8.

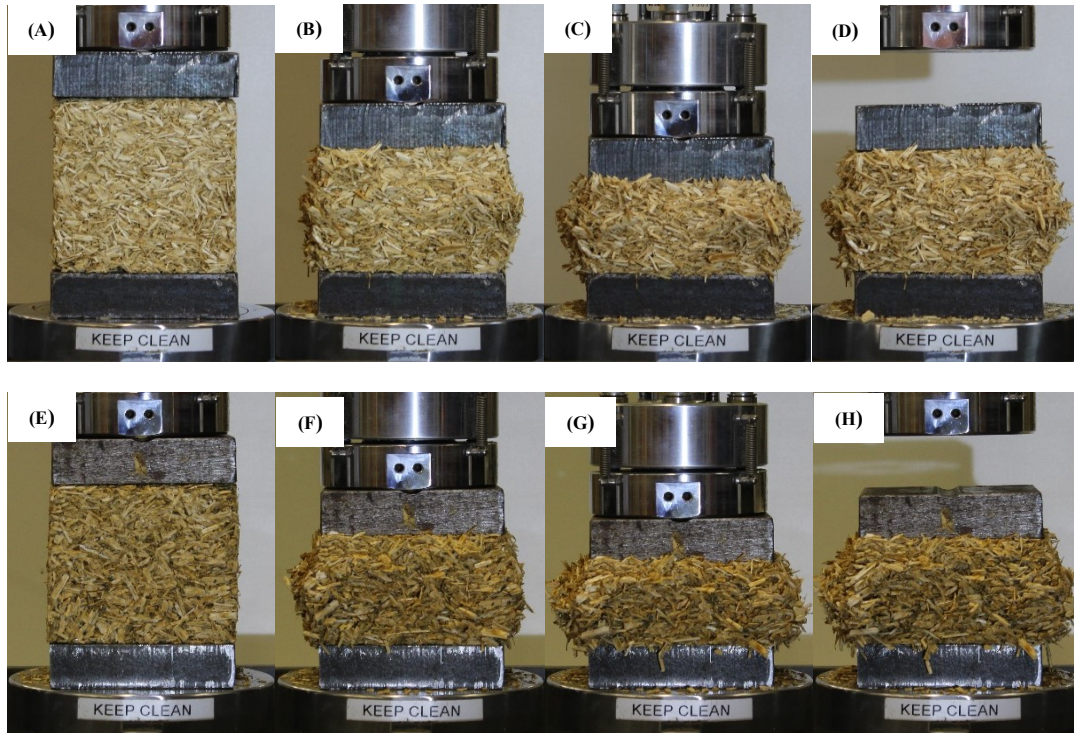


Figure 8. Compression testing of hemp shiv composites at; (A) 0% strain, (B) 30% strain, (C) 50% strain, (D) after 50% strain, and after immersion in water at (E) 0% strain, (F) 30% strain, (G) 50% strain, (H) after 50% strain.

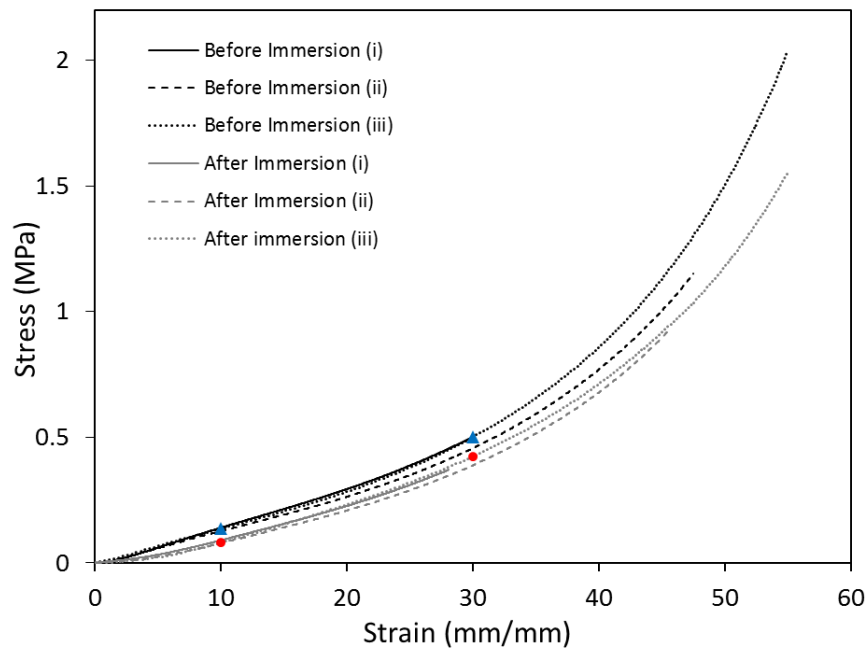


Figure 9. Compressive stress versus strain characteristics of hemp shiv composites before and after immersion in water.

4. Discussion

In the present study, hemp shiv based composites have been manufactured by using silica sol as a binder. The binding matrix has been characterised and its morphology, chemical composition and physical properties have been studied in comparison with silica glass. The binder is prepared by the hydrolysis and condensation of TEOS in water in the presence of ethanol as the mediator solvent. HDTMS is added for functionalisation thereby providing hydrophobic alkyl groups in the silica network. The formulation has been used earlier for treatment of hemp shiv particles for imparting hydrophobicity to the material [26]. Here we report the binding properties of silica when mixed with hemp shiv. The silica sol interacts with hemp shiv leaching out extractives and waxes which leads to visual changes turning the silica matrix from colourless transparent to yellowish opaque.

The silica is able to covalently bond to hemp shiv through the hydroxyl groups of cellulose [26]. During the drying process, the gel starts condensing, releasing ethanol and water and develops a silica network. The extracts from the shiv that are entrapped in the silica network alter the characteristics of the silica. From the SEM analysis, it was seen that the silica morphology is modified. The structure of the new modified silica with incorporated extracts is less brittle when compared to the pure silica glass.

The chemical composition of the silica specimens is mainly composed of carbon, oxygen and silicon. Chemical characterisation using EDX reveals that the modified silica (binding matrix) has a higher carbon content than the pure silica. Detailed XPS analysis indicates that due to sol interaction with hemp shiv, the silica chemistry has been significantly altered. The surface carbon content of the binding matrix increased by 27% (from 19% to 46%). On the other hand, the oxygen content decreased by 21% (from 61% to 40%). This change in C/O ratio and increase in the surface carbon content can be attributed to the additional extracts that have been identified in the modified network of the binding matrix. The decrease in surface oxygen content can be related to the masking effect of the hemp shiv extracts reducing the detectability of the oxygen bonds in the silica network.

336 The C1s high resolution XPS spectra reveal that the hemp shiv extracts have modified the silica
337 network leading to the appearance of C3 and C4 peaks which are not present in the pure silica
338 glass. Furthermore, the increase in the intensity of the C1 component for the binding matrix
339 from 68% to 84% indicates the presence of C-C and C-H bonds from the incorporated extracts.
340 To analyse the extracts that were leaching out from hemp shiv during the silica based
341 treatment, the process was simplified by using a solution of ethanol and water for the extraction
342 process. Ethanol is able to dissolve waxes and isolate lipophilic extractives. These ethanol-
343 soluble extractives were analysed using GCMS and it was found that the extract was mainly
344 composed of lauric acid and phthalic acid with many other fatty acids. The majority of the
345 compounds identified using GCMS belong to the group of lipophilic extractives which are
346 hydrophobic in nature [16,29]. This could possibly be one of the factors for the compatibility
347 between the lipophilic extractives and the sol-gel chemistry due to their hydrophobic nature.
348
349 The thermal decomposition patterns of the silica specimens were studied by TGA. The binding
350 matrix had a higher weight loss below 100 °C and a greater endothermic peak that can be
351 attributed to the presence of fatty acids in addition to the physically adsorbed water [30]. The
352 embedded extracts in the silica network changed the decomposition range of the organic
353 fragments of the silane corresponding to the temperature range of 270-600 °C [31]. Due to the
354 higher percentage of the organic compounds in the binding matrix, the weight loss was greater
355 and a peak shift was observed in the first derivative of the weight loss thermogram (DTG). The
356 maximum decomposition rate in the DTG curve for silica glass was at 520 °C attributed to the
357 loss of silanol groups. The modification of silica network with hemp shiv extracts lowered the
358 thermal stability of the binding matrix.
359
360 Composites were prepared using hemp shiv and silica sol and their mechanical performance
361 was evaluated. The composites were light weight with a density of 175 kg/m³ and the
362 compressive stress of 0.48 MPa attained at 30% strain is relatively good when compared to
363 other hemp shiv based composites such as hemp-lime (0.02 - 0.39 MPa at density 360 kg/m³)
364 [32], hemp-starch (0.4 MPa at density 177 kg/m³) [33] and hemp-clay (0.39 at density 373
365 kg/m³) [34]. Higher strains corresponded with higher compressive stresses leading to

densification of the sample without reaching a failure point. This suggests that the interfacial adhesion between the shiv and binding matrix is good and the shear forces are low.

After the immersion test, the decrease in mechanical strength can be related to the swelling of the shiv when placed in water for 24 hours. Since the binder also provides hydrophobicity to the hemp shiv, the compressive stress versus strain characteristics are not compromised to a great extent. However, the swelling could be related to the slow penetration of water through micro-cracks on the coated surface or due to the presence of small uncovered pores within the hemp shiv. The binder can provide hydrophobicity to the hemp shiv but it cannot fully protect the hemp shiv against long-term water interaction. The slight decrease in compressive stress reached at 30% strain can be attributed to the weakening of the interfacial bonding between the hemp shiv and the binding matrix. However, composites produced using an ethanol-water mixture instead of silica sol was unsuccessful as the hemp shiv fell apart on demoulding. The ethanol is responsible for isolation of the extractives and waxes from hemp shiv but the extractives cannot bind hemp shiv on their own. The extractives modify the silica chemistry and the binding matrix holds the hemp particles together resulting in the production of coherent composite blocks.

When compared to conventional hemp-lime composites, it is evident that the production costs of the hemp-silica composites would be higher due to the hydrophobic treatment on hemp shiv. However, this cost could be off-set by savings elsewhere, both in production ingredients (reduction in water usage, lower drying times) as well as an extension in service life, potentially reducing the whole life cost. Moreover, the commercial availability of sol-gel solution on an industrial scale would significantly lower the cost of this novel composite. The preparation of hemp-silica composite results in the reduction of 2L of mixing water per 1kg of hemp shiv when compared to a conventional hemp-lime composite. The thermal performance of the new composite is expected to be better due to their significantly lower density than hemp-lime. Overall early indications are that the global warming potential of this composite would be approximately 5% lower than that of a conventional composite. The life span is expected to increase by 50% due the improved resistance to water that is responsible for degradation of the composite.

5. Conclusions

In this work, the novel use of sol-gel treatment as a binding agent has been identified, providing multi-functionality from a single treatment using a simple, economical one-step process. Thorough investigation of the binder and its chemical interaction with hemp shiv has been performed. Lipophilic extractives from the shiv are integrated within the silica network, modifying chemical, morphological and physical characteristics of the glass material. The prepared composites show good mechanical performance as a non-load bearing material and has great potential as a thermal insulation material due to their low density as well as the high porosity of hemp shiv. Durability tests evaluated the robustness of the composite and the hydrophobic silica treatment was seen to enhance the water resistance of the material. This study is applicable to not only the hemp shiv material but also to any bio-based material which has cellulose and lipophilic extractives in its composition. This therefore transforms the current use of the sol-gel treatment as a surface modifier agent alone to dual functionality as a binder agent leading to economical and sustainable bio-based building materials.

Acknowledgments

This study was supported by the ISOBIO project funded by the Horizon 2020 programme [grant number 636835 – ISOBIO – H2020-EeB-2014-2015] and the Canadian Queen Elizabeth II Diamond Jubilee Scholarship. The authors would also like to acknowledge the EPSRC Centre for Decarbonisation of the Built Environment (dCarb) [grant number EP/L016869/1]. The contents of this publication are the sole responsibility of the authors and cannot be taken to reflect the views of the European Union. All data are provided in full in the results section of this paper.

Disclosure statement

The authors declare that they have no conflict of interest.

References

[1] Tran Le AD, Maalouf C, Mai TH, Wurtz E, Collet F. Transient hygrothermal behaviour of

426 a hemp concrete building envelope. *Energy Build* 2010;42:1797–806.
 427 doi:10.1016/j.enbuild.2010.05.016.

428 [2] Latif E, Lawrence M, Shea A, Walker P. Moisture buffer potential of experimental wall
 429 assemblies incorporating formulated hemp-lime. *Build Environ* 2015;93:199–209.
 430 doi:10.1016/j.buildenv.2015.07.011.

431 [3] Benfratello S, Capitano C, Peri G, Rizzo G, Scaccianoce G, Sorrentino G. Thermal and
 432 structural properties of a hemp-lime biocomposite. *Constr Build Mater* 2013;48:745–54.
 433 doi:10.1016/j.conbuildmat.2013.07.096.

434 [4] Shea A, Lawrence M, Walker P. Hygrothermal performance of an experimental hemp-
 435 lime building. *Constr Build Mater* 2012;36:270–5.
 436 doi:10.1016/j.conbuildmat.2012.04.123.

437 [5] Theis M, Grohe B. Biodegradable lightweight construction boards based on
 438 tannin/hexamine bonded hemp shaves. *Holz Als Roh - Und Werkst* 2002;60:291–6.
 439 doi:10.1007/s00107-002-0306-0.

440 [6] Jiang Y, Lawrence M, Ansell MP, Hussain A. Cell wall microstructure, pore size
 441 distribution and absolute density of hemp shiv. *R Soc Open Sci* 2018;5:171945.
 442 doi:10.1098/rsos.171945.

443 [7] Gassan J, Gutowski VS, Bledzki AK. About the surface characteristics of natural fibres.
 444 *Surf Eng* 2000;283:132–9. doi:10.1002/1439-2054(20001101)283:1<132::AID-
 445 MAME132>3.0.CO;2-B.

446 [8] Elfordy S, Lucas F, Tancret F, Scudeller Y, Goudet L. Mechanical and thermal properties
 447 of lime and hemp concrete (“hempcrete”) manufactured by a projection process. *Constr*
 448 *Build Mater* 2008;22:2116–23. doi:10.1016/j.conbuildmat.2007.07.016.

449 [9] Ahmad MR, Bing C, Oderji SY, Mohsan M. Development of a new bio-composite for
 450 building insulation and structural purpose using corn stalk and magnesium phosphate
 451 cement; Physical, mechanical, thermal and hygric evaluation. *Energy Build* 2018.
 452 doi:10.1016/j.enbuild.2018.06.007.

453 [10] Marceau S, Glé P, Guéguen-Minerbe M, Gourlay E, Moscardelli S, Nour I, et al.
 454 Influence of accelerated aging on the properties of hemp concretes. *Constr Build Mater*
 455 2017;139:524–30. doi:10.1016/j.conbuildmat.2016.11.129.

- 456 [11] Kidalova L, Stevulova N, Terpakova E. Influence of water absorption on the selected
457 properties of hemp hurds composites. Pollack Period 2015.
458 doi:10.1556/Pollack.10.2015.1.12.
- 459 [12] Gandolfi S, Ottolina G, Riva S, Fantoni GP, Patel I. Complete chemical analysis of
460 carmagnola hemp hurds and structural features of its components. BioResources
461 2013;8:2641–56. doi:10.15376/biores.8.2.2641-2656.
- 462 [13] PETTERSEN RC. The Chemical Composition of Wood 1984:57–126. doi:10.1021/ba-
463 1984-0207.ch002.
- 464 [14] Yang G, Jaakkola P. Wood chemistry and isolation of extractives from wood. Lit Study
465 BIOTULI Proj Univ Appl Sci 2011:10–22.
- 466 [15] S. M, D. Santana ALB, A. C, S. L, Bieber L. Phenolic Extractives and Natural Resistance
467 of Wood. Biodegrad - Life Sci 2013. doi:10.5772/56358.
- 468 [16] Sun RC, Tomkinson J. Comparative study of organic solvent-soluble and water-soluble
469 lipophilic extractives from wheat straw 2: Spectroscopic and thermal analysis. J Wood
470 Sci 2002;48:222–6. doi:10.1007/BF00771371.
- 471 [17] Gutiérrez A, Del Río JC, Martínez MJ, Martínez AT. The biotechnological control of pitch
472 in paper pulp manufacturing. Trends Biotechnol 2001;19:340–8. doi:10.1016/S0167-
473 7799(01)01705-X.
- 474 [18] Kabir MM, Wang H, Lau KT, Cardona F, Aravinthan T. Mechanical properties of
475 chemically-treated hemp fibre reinforced sandwich composites. Compos Part B Eng
476 2012;43:159–69. doi:10.1016/j.compositesb.2011.06.003.
- 477 [19] Xie Y, Hill CAS, Xiao Z, Militz H, Mai C. Silane coupling agents used for natural
478 fiber/polymer composites: A review. Compos Part A Appl Sci Manuf 2010;41:806–19.
479 doi:10.1016/j.compositesa.2010.03.005.
- 480 [20] Pickering KL, Efendy MGA, Le TM. A review of recent developments in natural fibre
481 composites and their mechanical performance. Compos Part A Appl Sci Manuf
482 2016;83:98–112. doi:10.1016/j.compositesa.2015.08.038.
- 483 [21] Valadez-Gonzalez A, Cervantes-Uc JM, Olayo R, Herrera-Franco PJ. Effect of fiber
484 surface treatment on the fiber-matrix bond strength of natural fiber reinforced
485 composites. Compos Part B Eng 1999;30:309–20. doi:10.1016/S1359-8368(98)00054-7.

- 486 [22] Sepe R, Bollino F, Boccarusso L, Caputo F. Influence of chemical treatments on
487 mechanical properties of hemp fiber reinforced composites. *Compos Part B Eng*
488 2018;133:210–7. doi:10.1016/J.COMPOSITESB.2017.09.030.
- 489 [23] Sullins T, Pillay S, Komus A, Ning H. Hemp fiber reinforced polypropylene composites:
490 The effects of material treatments. *Compos Part B Eng* 2017;114:15–22.
491 doi:10.1016/j.compositesb.2017.02.001.
- 492 [24] Kabir MM, Wang H, Lau KT, Cardona F. Chemical treatments on plant-based natural
493 fibre reinforced polymer composites: An overview. *Compos Part B Eng* 2012;43:2883–
494 92. doi:10.1016/j.compositesb.2012.04.053.
- 495 [25] Da Silva LJ, Panzera TH, Velloso VR, Christoforo AL, Scarpa F. Hybrid polymeric
496 composites reinforced with sisal fibres and silica microparticles. *Compos Part B Eng*
497 2012;43:3436–44. doi:10.1016/j.compositesb.2012.01.026.
- 498 [26] Hussain A, Calabria-Holley J, Schorr D, Jiang Y, Lawrence M, Blanchet P.
499 Hydrophobicity of hemp shiv treated with sol-gel coatings. *Appl Surf Sci* 2018;434:850–
500 60. doi:10.1016/j.apsusc.2017.10.210.
- 501 [27] Hussain A, Calabria-Holley J, Jiang Y, Lawrence M. Modification of hemp shiv properties
502 using water-repellent sol-gel coatings. *J Sol-Gel Sci Technol* 2018. doi:10.1007/s10971-
503 018-4621-2.
- 504 [28] Marques G, del Río JC, Gutiérrez A. Lipophilic extractives from several nonwoody
505 lignocellulosic crops (flax, hemp, sisal, abaca) and their fate during alkaline pulping and
506 TCF/ECF bleaching. *Bioresour Technol* 2010;101:260–7.
507 doi:10.1016/j.biortech.2009.08.036.
- 508 [29] Hardell HL, Nilvebrant NO. A rapid method to discriminate between free and esterified
509 fatty acids by pyrolytic methylation using tetramethylammonium acetate or hydroxide. *J*
510 *Anal Appl Pyrolysis* 1999;52:1–14. doi:10.1016/S0165-2370(99)00035-2.
- 511 [30] Knothe G, Dunn RO. A Comprehensive Evaluation of the Melting Points of Fatty Acids
512 and Esters Determined by Differential Scanning Calorimetry. *J Am Oil Chem Soc*
513 2009;86:843–56. doi:10.1007/s11746-009-1423-2.
- 514 [31] Hemsri S, Asandei AD, Grieco K, Parnas RS. Biopolymer composites of wheat gluten
515 with silica and alumina. *Compos Part A Appl Sci Manuf* 2011;42:1764–73.

516 doi:10.1016/j.compositesa.2011.07.032.

517 [32] Walker R, Pavia S, Mitchell R. Mechanical properties and durability of hemp-lime
518 concretes. *Constr Build Mater* 2014;61:340–8. doi:10.1016/j.conbuildmat.2014.02.065.

519 [33] Benitha Sandrine U, Isabelle V, Ton Hoang M, Maalouf C. Influence of chemical
520 modification on hemp-starch concrete. *Constr Build Mater* 2015;81:208–15.
521 doi:10.1016/j.conbuildmat.2015.02.045.

522 [34] Mazhoud B, Collet F, Pretot S, Lanos C. Mechanical properties of hemp-clay and hemp
523 stabilized clay composites. *Constr Build Mater* 2017;155:1126–37.
524 doi:10.1016/j.conbuildmat.2017.08.121.

525